Biomacromolecules

pubs.acs.org/Biomac

Article

Sugar-Assisted Cryopreservation of Stem Cell-Laden Gellan Gum–Collagen Interpenetrating Network Hydrogels

Jian Yao Ng, Kee Ying Fremi Tan, and Pui Lai Rachel Ee*

Cite This: *Biomacromolecules* 2022, 23, 2803–2813

Read Online

ACCESS | Metrics & More | Article Recommendations | Supporting Information

ABSTRACT: Tissue engineering involves the transplantation of stem cell-laden hydrogels as synthetic constructs to replace damaged tissues. However, their time-consuming fabrication procedures are hurdles to widespread application in clinics. Fortunately, similar to cell banking, synthetic tissues could be cryopreserved for subsequent central distribution. Here, we report the use of trehalose and gellan gum as biomacromolecules to form a cryopreservable yet directly implantable hydrogel system for adipose-derived stem cell (ADSC) delivery. Through a modified cell encapsulation method and a preincubation step, adequate cryoprotection was afforded at 0.75 M trehalose to the encapsulated ADSCs. At this concentration, trehalose demonstrated lower propensity to induce apoptosis than 10% DMSO, the current gold standard cryoprotectant. Moreover, when cultured along with trehalose after thawing, the encapsulated ADSCs retained their stem cell-like phenotype and osteogenic differentiation capacity. Taken together, this study demonstrates the feasibility of an "off-the-shelf" biomacromolecule-based synthetic tissue to be applied in widespread tissue engineering applications.

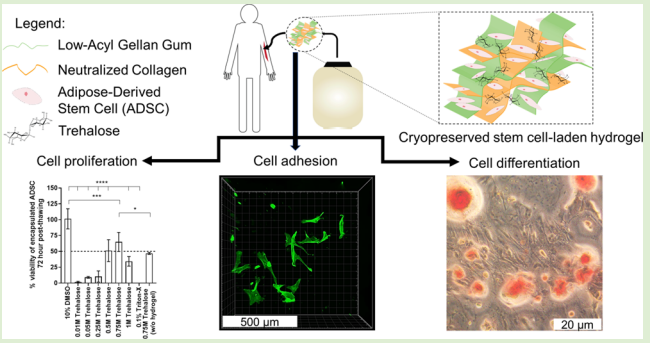

1. INTRODUCTION

Tissue engineering and regenerative medicine (TERM) has proven to be efficacious in a wide range of therapeutic areas such as cardiovascular diseases, bone/cartilage-related diseases, and inflammatory conditions.[1] Using synthetic tissues, TERM technologies provide substitutes to replace or repair damaged anatomy. For the fabrication of synthetic tissues, the current clinical practice involves a time-consuming laboratory-based process of cell expansion and encapsulation into a 3D scaffold, which has to be repeated every time upon receiving a request.[2] This demands for substantial resources and is a quantum barrier to the widespread clinical translation of TERM. To overcome this issue, many envision an "off-the-shelf" synthetic tissue construct product that can be fabricated and cryopreserved in its entirety for subsequent central distribution, after which the cryopreserved constructs can be transported and directly implanted at the clinics after thawing (Figure 1). In order to achieve this, the prerequisite is to develop a cryopreservable 3D tissue construct using a nontoxic cryoprotectant.

Cryopreservation halts the metabolic activity of cells by putting them in cryogenic temperatures of −153 to −196 °C,[3] hence allowing the long-term storage of cells for subsequent usage.[4] The freeze−thaw process is known to induce mechanical injury to cells, owing to intracellular ice formation (IIF) and abrupt osmotic changes when water molecules crystallize.[5] Hence, dimethyl sulfoxide (DMSO) at 10% (v/v) is conventionally added as an essential cryoprotectant to minimize these damages. However, DMSO is toxic to humans at room temperature,[6] and adverse events such as nausea, vomiting,[7,8] cardiac syndromes,[9] and even cases of neurotoxicity[10,11] have been reported for patients implanted with cells cryopreserved with DMSO. The membrane permeabilizing effect of DMSO disrupts the normal diffusion gradients controlling cellular homeostasis.[12] In principle, most of the commonly used cryoprotective agents (CPAs) such as DMSO and glycerol need to penetrate the cells to minimize IIF and consequently exhibit cytotoxic effects to varying extents.[13]

In recent years, nontoxic polysaccharide-based alternative CPAs have been reported to yield adequate cryoprotection.[6] Among these alternatives, trehalose, a nontoxic disaccharide, has stood out given its superior ability to interact with water molecules.[14] When added as an adjuvant, trehalose reduced the concentration of DMSO required for cryopreserving multiple cell types and tissues.[15,16] However, cells cryopreserved solely with trehalose achieved lower viability upon thawing compared to DMSO.[17] This is because trehalose is mechanistically a noncell penetrating CPA.[18] Without modifications, trehalose

Received: February 9, 2022
Revised: May 17, 2022
Published: June 8, 2022

https://doi.org/10.1021/acs.biomac.2c00176
Biomacromolecules 2022, 23, 2803−2813

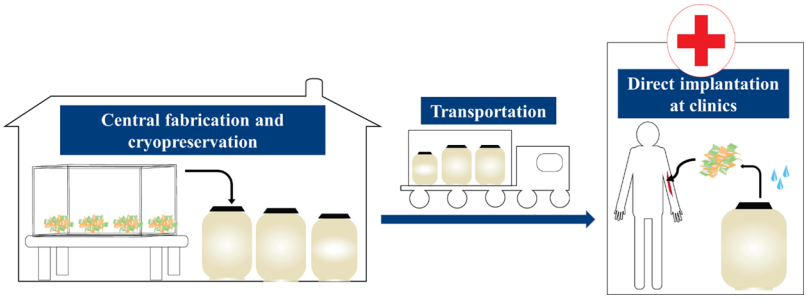

Figure 1. New TERM paradigm. A cryopreservable synthetic tissue construct will allow its central fabrication, delivery, and direct implantation at the clinics. Such an off-the-shelf variant eliminates the need for laboratory-based procedures and hence greatly increases the availability of TERM to patients. The choice of the cryoprotectant is an important consideration in order for the entire synthetic tissue to be biocompatible for implantation.

remains largely in the extracellular space and functions mainly by introducing a hyperosmotic cryomedium environment to draw out intracellular water and minimize IIF.[19] Yet, due to this noncell penetrating property, trehalose is highly tolerated by humans and can be administered without being removed after thawing.[20]

Hydrogel cryopreservation systems have another approach that researchers have utilized to cryopreserve cells with lower amounts of cytotoxic CPAs.[21] Encapsulated cells are less prone to ice injury as ice formation in the hydrogel microenvironment is limited.[22] In particular, hydrogels made up of polyanionic polymers provide enhanced cryoprotection as they attract water molecules better and are able to disrupt the water−ice interaction to restrict ice crystal growth.[12,23,24] Consequently, encapsulated cells were able to achieve comparable post-thaw cell viability using up to four times lower concentrations of DMSO.[25,26]

In a prior study, an interpenetrating network (IPN) hydrogel between collagen and gellan gum, a polyanionic microbial polysaccharide, has been developed to deliver adipose-derived stem cells (ADSCs) for tissue engineering application.[27] In comparison to other commonly used hydrogel-forming biomacromolecules such as agarose and xanthan gum, a milder condition of gelation facilitates the incorporation of cells, which allows gellan gum-based hydrogels to be studied for various TERM applications.[1] This attractive property has recently propelled gellan gum into a class of biomaterials of particular interest among researchers. Next, we sought to incorporate trehalose into the IPN hydrogel formula, exploiting the advantage that interactions between trehalose and a polyanionic hydrogel-forming polymer may enhance trehalose's cryoprotecting ability to disrupt the tetrahedral hydrogen bond network of ice crystals[28−30] and form a gellan gum-based hydrogel cryopreservation system employing trehalose as the sole CPA. Previous studies on hydrogel cryopreservation systems have indicated that numerous critical cryopreservation steps such as cell encapsulation, preincubation, and freezing procedures need to be optimized.[6] These convoluted procedures warrant for an in-depth research study.

Here, we unveiled a method to cryopreserve ADSCs encapsulated within a gellan gum-based hydrogel tissue construct using trehalose as the sole CPA. Advantageous cryopreservation steps to infuse trehalose into the ADSC-laden hydrogel matrix were incorporated based on cryobiological perspectives. With our method, adequate post-thaw cell viability could be achieved with a trehalose concentration of 0.75 M. Without the removal of trehalose, the post-thaw ADSCs adhered to the hydrogel matrix, expressed a stem cell-like phenotype, and were successfully induced to differentiate down the osteogenic pathway. Collectively, this study reports the development of an off-the-shelf synthetic tissue, harnessing synergism between the natural functions of carbohydrate polymers to engineer a clinically relevant TERM construct, without introducing potentially harmful materials with synthetic chemistry.

2. MATERIALS AND METHODS

2.1. Materials. Trehalose powder (D-(+)-trehalose dihydrate, 11936901) was obtained from Acros Organics. Low-acyl gellan gum (Gelzan CM, G1910), magnesium chloride ($MgCl_2$, 208337), sodium hydroxide (NaOH, S8045), sodium bicarbonate ($NaHCO_3$, S5761), hydrochloric acid (HCl, 320331), low-glucose Dulbecco's modified Eagle's medium (DMEM, D5523), Accutase solution (A6964), penicillin/streptomycin (P4333), paraformaldehyde (PFA, P6148), 2-phosphate L-ascorbic acid trisodium salt (49752), dexamethasone (D4902), β-glycerophosphate disodium salt hydrate (G9422), and cetylpyridinium chloride (CPC, C0732) were purchased from Sigma-Aldrich (St Louis, MO, USA). DMSO (200001-612) was obtained from VWR Singapore Pte Ltd. (Singapore). Type-1 rat tail collagen (SC-136157) was acquired from Santa Cruz Biotechnology, Inc. (Dallas, TX, USA). Ultrapure grade phosphate buffered saline (10× PBS) was purchased from Vivantis Technologies Sdn Bhd (Subang Jaya, Selangor Darul Ehsan, Malaysia). Trypan blue in 0.4% PBS solution (C838W29) and fetal bovine serum (FBS, SV30160.03) were bought from HyClone (South Logan, UT, USA). A CellTiter 96 AQueous One Solution Cell Proliferation Assay (MTS) kit was purchased from Promega (Madison, WI, USA). Alizarin red S (ARS, ab146374) and Phalloidin-iFluor 488 reagent (ab176753) were secured from Abcam (Cambridge, UK). Triton-X was obtained from Bio-Rad Laboratories (Hercules, CA, USA). ADSCs (PT-5006) were acquired from Lonza Bioscience (Basel, Switzerland). Polyethersulfone (PES, 0.22 μm) filters were procured from Sartorius AG (Göttingen, Germany). All other materials obtained were of research grade and used as received.

2.2. Methods. *2.2.1. Fabrication of Cryopreservable off-the-Shelf Synthetic Tissues. 2.2.1.1. Preparation of the Gellan Gum−Collagen IPN Hydrogels.* The hydrogel was prepared as previously described.[27] Briefly, gellan gum and $MgCl_2$ powders were separately dissolved in deionized water to form their respective aqueous solutions. Gellan gum solutions were always first progressively heated to 90 °C and kept at this temperature for 30 min for polymer chains to untangle into random coils. A completely homogeneous solution should be obtained if gellan gum polymers were completely dissolved. Subsequently, gellan gum solutions were cooled to 37 °C and maintained at this temperature until further use. A neutralized type-1 collagen solution was prepared to a final concentration of 3.33 mg/mL using 10× PBS, 1 N NaOH, and double distilled water ($_{dd}H_2O$) according to the manufacturer's protocol. The neutralized collagen solution was kept ice-cold and used within 2−3 h of preparation.

https://doi.org/10.1021/acs.biomac.2c00176
Biomacromolecules 2022, 23, 2803−2813

Gellan gum−collagen hydrogels were prepared by mixing sterile gellan gum and neutralized collagen to form a gel precursor within a 2 mL cryogenic vial (Corning, NY, USA). $MgCl_2$ solution was then added to the gel precursor to form 200 μL of hydrogel per cryovial. The final optimized concentrations of gellan gum, collagen, and $MgCl_2$ were 0.4% (w/v), 1 mg/mL, and 0.02% (w/v), respectively. Hydrogels were then incubated for 30 min at 37 °C to allow for collagen fibrinogenesis. Thereafter, the hydrogels were transferred to a −80 °C freezer and frozen for a minimum duration of 2 h. After freezing, they were dried overnight using a freeze-dryer (Alpha 1-2 LD +, Christ Martin, Germany) at −55 °C and 0.040 mbars. The dried hydrogels within cryovials were sterilized with bactericidal UV light for 2 h prior to use.

2.2.1.2. Encapsulation of ADSCs into the Gellan Gum−Collagen IPN Hydrogels. Cryomedia were always prepared fresh and used within 3 days of reconstitution. Briefly, trehalose powder (D-(+)-trehalose dihydrate) was weighed and dissolved in basal culture media to give final concentrations of 0.01, 0.05, 0.25, 0.5, 0.75, and 1 M. Cryomedia containing 10% (v/v) DMSO were made by adding 300 μL of DMSO to 2.7 mL of basal cell culture media. All cryomedia were sterile-filtered using 0.22 μm PES filters.

Frozen ADSCs placed in cryovials were thawed and cultured on Nunc T-75 cell culture flasks (Roskilde, Denmark) according to the manufacturer's protocol. Stem cell expansion was performed under basal conditions using 90% (v/v) low-glucose DMEM supplemented with 10% (v/v) FBS and 1% (v/v) penicillin−streptomycin. The culture media were replaced every two−3 days. Stem cells between passages 3 and 6 were used. All cells were harvested between 80 and 90% confluency.

To harvest cells, ADSCs were incubated with Accutase solutions at 37 °C in a humidified atmosphere of 5% CO_2 in air for 5 min. Cell densities were counted using 10 μL of cell suspension each with trypan blue staining to distinguish between live and dead cells. After centrifugation at 200 × g for 5 min, the cell pellets were resuspended with appropriate volume of cryomedia to achieve a density of 1×10^3 cells/μL of cryomedia. The cell-laden hydrogels were then fabricated by adding 200 μL of the cell suspension into each of the freeze-dried hydrogel. Through a modified cell encapsulation process, the hydrogels were then incubated for 30 min at 120 rpm to allow for hydrogel swelling, ADSC encapsulation, and for trehalose to be preincubated with ADSCs before freezing.

2.2.1.3. Cryopreservation Process. The cell-laden hydrogels were cryopreserved at a controlled rate of −1 °C/min to −80 °C using an isopropanol-filled freezing container (Nalgene, Rochester, NY, USA). The cryovials were then subjected to liquid nitrogen flow for overnight cooling to −196 °C. The cryopreserved ADSC-laden hydrogels were kept in this condition for at least 3 days (Scheme 1). For cell recovery, the ADSC-laden hydrogels were rapidly thawed by rewarming in a 37 °C water bath, and the thawed cell-laden hydrogels were directly transferred into each well of 24-well plates and prefilled with 400 μL of fresh culture media. The cryoprotectant was not removed, and the ADSCs within the hydrogels were cultured at 37 °C in humidified air with 5% CO_2. If the culture duration exceeded 3 days, the spent media were replaced every 2 to 3 days (Monday, Wednesday, and Friday).

2.2.2. Physical Characterization. 2.2.2.1. Rheometry. Rheometric analysis of the hydrogels was performed with an oscillatory rheometer (MCR 302, Antor Paar, Austria) using a plate-plate geometry (diameter = 8 mm and working gap = 1 mm). Amplitude and frequency sweep tests were conducted on hydrogels immediately after fabrication and after freeze-drying, which were then incubated and rehydrated with basal culture media, respectively. The aim was to determine if the freeze-drying process altered the internal structure of the hydrogel significantly. Measurements were carried out using three different samples (n = 3) with sufficient hydrogel to fill the gap in each run. All measurements were conducted at 25 °C.

The linear viscoelastic (LVE) region of each hydrogel sample was first determined via amplitude sweeps. Storage (G′) and loss (G″) moduli were obtained between the range of 0.1 to 100% shear strain at a constant frequency of 1 Hz. The linearity limit was determined

Scheme 1. Schematic Representation of the Fabrication and Cryopreservation of Trehalose-Infused ADSC-Laden Gellan Gum−Collagen Hydrogels[a]

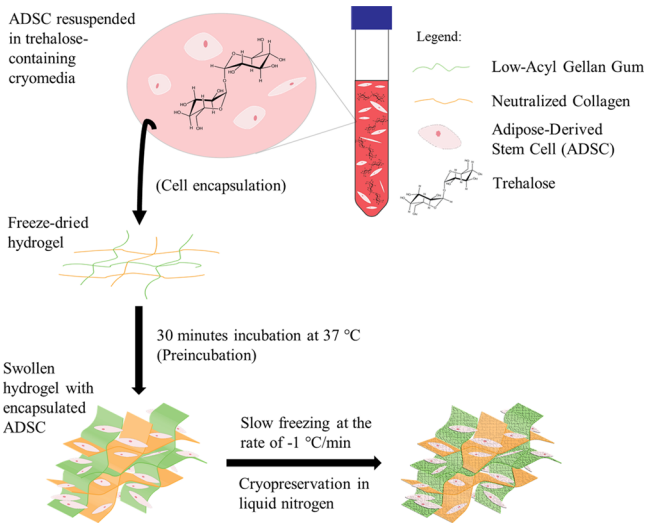

[a]ADSCs resuspended in cryomedia containing trehalose were incorporated into the freeze-dried hydrogel network for cell encapsulation. Next, the trehalose-infused ADSC-laden hydrogels were preincubated for 30 min at 37 °C and then cryopreserved in their entirety at an optimal cooling rate of −1 °C/min to −80 °C, after which the frozen tissue constructs were subjected to liquid nitrogen flow for cryostorage. The cryopreserved tissue construct is intended for direct implantation (including the cryoprotectant) after thawing, without the need for further laboratory-based manipulation at the clinics.

using a straight ruler on the graph plotted. Next, the stability of the hydrogel structures under different rates of motions was studied via frequency sweeps. G′ and G′′ moduli measurements were completed from minimum to maximum frequency between 0.01 and 10 Hz. The shear strain was set to a constant value within the predetermined LVE region.

2.2.2.2. Microcomputed Tomography (μCT). The 3D porosity of hydrogels before and after freeze-drying was examined and compared using X-ray microcomputed tomography. Hydrogel samples were scanned using a Quantum FX microCT scanner (PerkinElmer, Waltham, MA, USA). Scans were conducted in the highest resolution mode of 4.5 min per scan using a pixel size of 10 μm and 90 kV of energy with 0.16 mA of current. Representative 513 slices of images for each sample were stacked to give a volumetric rendering 3D view using AMIDE v1.0.5.

2.2.2.3. Gravimetric Analysis for Swelling Ratio and Degradation Profile. To determine the swelling ratio, each of the 200 μL of freeze-dried hydrogels was weighed (W_i) and separately transferred into 15 mL Falcon tubes (n = 3). The hydrogels were immersed in 1 mL of cryomedia containing 0.75 M trehalose and incubated at 37 °C under constant agitation of 120 rpm (MaxQ 4000, Thermo Fisher Scientific, Waltham, MA, USA). At predetermined time points, the supernatant was decanted, and the mass of hydrogels was blot-dried and reweighed (W_{sw}). The percentage mass increase of the hydrogels due to hydrogel swelling was calculated according to eq 1. Fresh 1 mL of cryomedia was replenished after each time point.

$$\%\text{mass increase} = \left(\frac{W_{sw}}{Wi}\right) \times 100\% \quad (1)$$

After the hydrogels reached their equilibrium swelling capacity (W_o), they were further examined for degradation in terms of mass loss for up to a total of 14 days. Similarly, at predetermined time points, the supernatant was decanted, and the remaining mass of hydrogels was blot-dried and reweighed (W_r). The remaining

https://doi.org/10.1021/acs.biomac.2c00176
Biomacromolecules 2022, 23, 2803−2813

percentage mass of the hydrogels was calculated according to eq 2. Similarly, 1 mL of fresh cryomedia was replenished after each time point.

$$\%\text{mass remaining} = \left(\frac{W_r}{W_o}\right) \times 100\% \quad (2)$$

2.2.3. Biological Characterization. 2.2.3.1. Viability of Cryopreserved ADSCs via the MTS Assay. After 72 h of culture, the spent media in all wells were removed and replaced with fresh culture media (n = 3), and MTS solution was added to each well at a 1:10 (MTS:media) volume ratio. The cell-laden hydrogels were then incubated with MTS for another 3 h, after which 100 μL of the supernatant mixture was removed from each well and transferred to a transparent, flat, round-bottom 96-well plate (Greiner Bio-One, flat transparent bottom) for absorbance reading at 490 nm absorbance using a Tecan Infinite M200 pro plate reader (Tecan, Männedorf, Switzerland) (A). Cell-free wells containing only cell culture media were treated as "blanks" (A_b). ADSCs treated with sterile-filtered 0.1% Triton-X were used as negative controls. Nonencapsulated ADSCs cryopreserved only with 0.75 M trehalose were used to determine if the presence of the IPN hydrogel cryopreservation system would increase the cell viability. All percentage viabilities were obtained by expressing their blank-corrected absorbance readings against those of cells cryopreserved within the hydrogel using 10% DMSO (A_c) [eq 3].

$$\%\text{cell viability} = \frac{A - A_b}{A_c - A_b} \times 100 \quad (3)$$

Cell viabilities were not expressed against an additional non-cryopreserved ADSC-laden hydrogel arm because cells exposed to cryopreservation and thawing could experience confounding cytotoxicity and osmotic effects from the processes, respectively. Therefore, comparison of the cell viabilities of encapsulated ADSCs cryopreserved with varying concentrations of trehalose to those of 10% DMSO directly would better address the primary aim of this study, which is to develop a method to incorporate trehalose as a cryoprotectant for the ADSC-laden gellan gum−collagen hydrogels and compare them to the 10% DMSO variants.

2.2.3.2. Enzyme-Linked Immunosorbent Assay (ELISA) of Human Active Caspase-3. Prolonged exposure to DMSO is known to induce apoptosis in mammalian cells.[31] After the cryopreserved ADSC-laden hydrogels were thawed (n = 3), the cells were cultured along with their cryoprotectant (10% DMSO or 0.75 M trehalose) for 48 h. Quantification of intracellular active caspase-3 was then conducted with an Abcam Human Active Caspase-3 Ser29 ELISA kit (ab181418, Cambridge, UK) according to the manufacturer's protocol. After the assay, the amount of intracellular active caspase-3 was measured using the Tecan Infinite M200 pro plate reader (Figure S1), and the values were divided by the amount of viable cells. The viability-corrected concentrations of caspase-3 served as a quantitative biomarker for the comparative number of viable ADSCs undergoing early apoptosis.[32]

2.2.3.3. Confocal Laser Scanning Microscopy (CLSM) of Cryopreserved ADSCs. To ascertain that the encapsulated ADSCs cryopreserved with 0.75 M trehalose were able to adhere and spread in a 3D fashion within the hydrogel matrix, z-stack confocal imaging of the F-actin-stained cells was conducted. ADSC-laden hydrogels, at the same cell density stated above, were thawed and cultured for 0, 7, and 14 days in each chamber of a Nunc 2-chamber borosilicate cover glass system (Roskilde, Denmark).

F-actin staining was conducted according to the manufacturer's protocol. Briefly, the encapsulated cells were first fixed with 4% PFA for 20 min and then permeabilized with 0.1% Triton-X for 5 min. Subsequently, the permeabilized cells were stained with 1× Phalloidin-iFluor 488 reagent for 75 min in the dark. The entire staining procedure was conducted at room temperature conditions. Confocal z-stack images were then captured with a Zeiss LSM710 (Oberkochen, Germany) using the 20×/0.8 objective lens with a 488 nm argon laser as the excitation source. Images were processed and exported using Imaris v9.5.3 (Bitplane, Zürich, Switzerland).

2.2.3.4. Phase-Contrast Imaging of Cryopreserved ADSCs. To qualitatively examine the effect of cryopreservation on encapsulated ADSCs using 10% DMSO, 0.5 M trehalose, or 0.75 M trehalose, the cell morphologies were imaged on days 1, 3, 5, 7, and 14 post-thawing using an inverted microscope (Olympus CKX41) along with its associated control box (Olympus DP21) (Olympus, Tokyo, Japan).

2.2.3.5. Flow Cytometry of Cryopreserved ADSCs. After 14 days of culture, the cell phenotype of encapsulated ADSCs cryopreserved with 0.75 M trehalose was assessed via flow cytometry using a CytoFLEX S flow cytometer (Beckman Coulter, CA, USA). Briefly, ADSCs were first harvested using the Accutase solution and resuspended in 1× PBS at a cell density of 1 × 10^6 cells/mL. The cell suspension was then divided into three equal portions and separately stained with FITC anti-human CD105 (Clone MEM-229), CD73 (Clone AD2), or CD90 (Clone 5E10). Next, all the cells were concurrently stained with secondary PE/Cy5.5 anti-human CD45 (Clone HI30) (all from Abcam, Cambridge, UK). Cells were stained at 4 °C for 15 min in the dark according to the manufacturer's protocol. Untreated and unstained ADSCs expressing negligible fluorescence were assessed in the same manner for the quadrants to be drawn. The percentage of positive cells for each marker was averaged from three independent experiments (n = 3).

2.2.3.6. Osteogenic Differentiation of Cryopreserved ADSCs. Cryopreserved ADSC-laden hydrogels were thawed and cultured for 7 days under basal conditions to allow for cell adhesion and proliferation until 90% confluency was achieved. Subsequently, osteogenic induction was initiated by replacing the basal media with osteogenic media. Osteogenic media were prepared by supplementing basal media with 100 nM dexamethasone, 50 μM 2-phosphate L-ascorbic acid, and 10 mM β-glycerophosphate. Experiments were conducted in duplicates for different trehalose concentrations with parallel wells in basal media used as negative controls (n = 2). Blank controls were cell-free hydrogels incubated in basal media and osteogenic media. Osteogenesis was induced for a total of 14 days. All wells were replaced with respective fresh basal or osteogenic media every two to 3 days (Monday, Wednesday, and Friday).

Alizarin Red S (ARS) Staining: Successful osteogenesis of the encapsulated ADSCs was indicated by the presence of calcium deposits secreted by newly formed osteocytes in the process of ECM mineralization. Alizarin red S (ARS) staining was conducted to specifically bind to and identify these calcium deposits. Briefly, the cells were first fixed with 4% PFA solution for 30 min and then subjected to ARS staining in the dark, with 2% (w/v) ARS solution corrected to pH 4.1−4.3, for 45 min. Images of stained calcium deposits along with fixed cells were captured using an inverted microscope (Olympus CKX41) along with its associated control box (Olympus DP21) (Olympus, Tokyo, Japan).

ARS Quantification via CPC Extraction: To quantify the amount of ARS-stained calcium deposits, 10% CPC buffered solution (pH 7.4) was added for 15 min with mild agitation (120 rpm) for extraction, after which 100 μL of the supernatant mixture was removed from each well and transferred to a transparent, flat, round-bottom 96-well plate (Greiner Bio-One, flat transparent bottom) to measure absorbance at 570 nm using the Tecan Infinite M200 pro plate reader.

Alkaline Phosphatase (ALP) Assay: ALP is an enzyme expressed during bone mineralization.[33] After thawing, osteogenesis was induced for 5 days as described above, after which intracellular ALP was quantified using an ALP assay kit (ab83371, Abcam) according to the manufacturer's protocol. Briefly, cell lysates were incubated within each well of an opaque, flat, round-bottom 96-well plate (Corning, NY, USA). The presence of ALP cleaves the phosphate group of the nonfluorescent 4-methylumbelliferyl phosphate disodium salt assay substrate into fluorescent 4-methylumbelliferone (4-MU). The fluorescence intensity of 4-MU was measured at Ex/Em = 360/440 nm using the Tecan Infinite M200 pro plate reader and quantified using standards (Figure S2).

2.2.4. Statistical Analysis. All statistical analyses were conducted with GraphPad Prism v8.4.3. The data are presented as mean ± standard deviation (SD). p values were calculated using independent sample unpaired t tests. $^{ns}p > 0.05$ was considered statistically

https://doi.org/10.1021/acs.biomac.2c00176
Biomacromolecules 2022, 23, 2803−2813

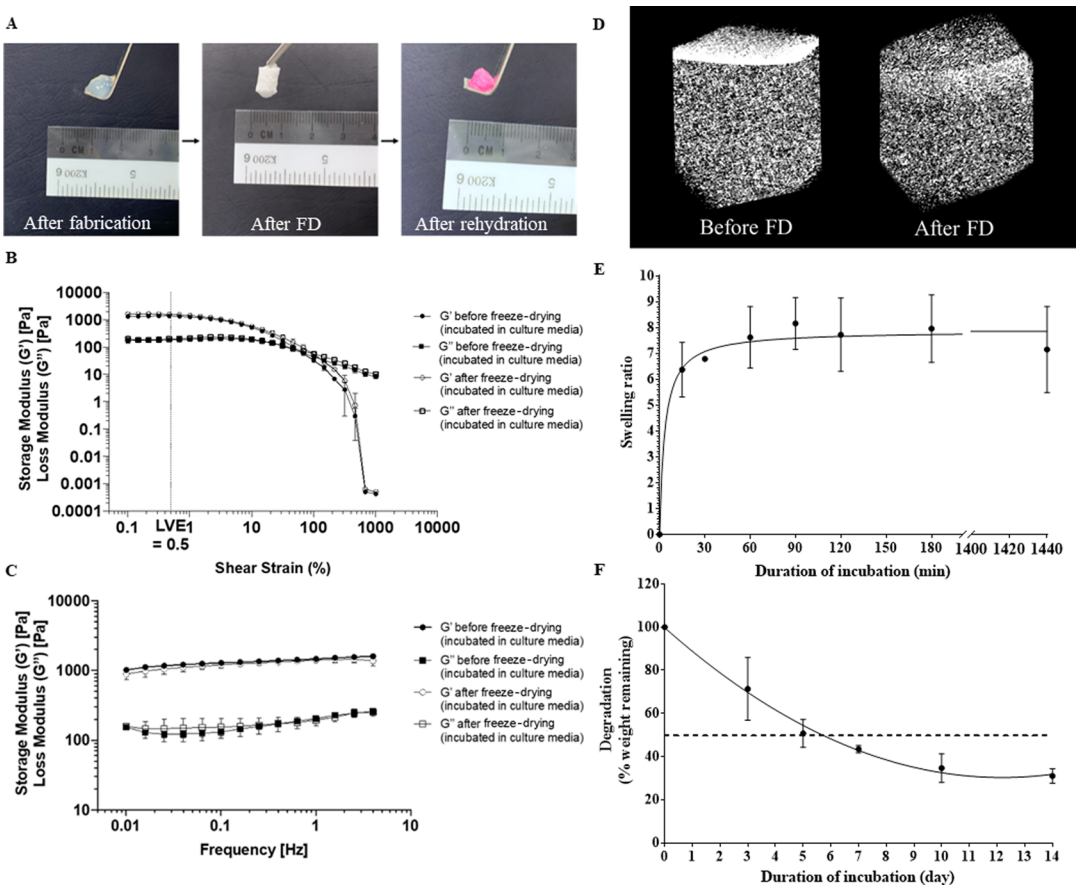

Figure 2. Physical characterization of the cryopreservable hydrogel system. (A) Gross visual images of hydrogels immediately after fabrication, immediately after freeze-drying (FD), and immediately after rehydration with basal cell culture media. (B) Rheological properties of the hydrogels before and after freeze-drying. Amplitude sweeps were conducted to identify the hydrogels' limit of LVE. (C) Frequency sweeps were conducted, within the range of LVE, to determine the hydrogels' viscoelastic properties as a function of shear frequency. For both plots, storage modulus (G′) [Pa] and loss modulus (G″) [Pa] against shear strain [%] or frequency [Hz] are presented (mean ± SD and $n = 3$). (D) Reconstructed 3D μCT images of hydrogels before and after FD. The 3D replicas were generated from 513 slices of flat 2D images using volume rendering. (E) Swelling ratio and (F) degradation profiles of hydrogels incubated in cryomedia containing 0.75 M trehalose (mean ± SD and $n = 3$).

nonsignificant; *$p < 0.05$ was considered statistically significant. Other symbols considered as significant were denoted as follows **$p < 0.01$; ***$p < 0.001$; and ****$p < 0.0001$.

3. RESULTS AND DISCUSSION

3.1. Physical Properties of Gellan Gum−Collagen IPN Hydrogels before and after Freeze-Drying. *3.1.1. Rheological Properties.* Cell encapsulation is a procedure that exposes ADSCs to nonphysiological conditions and induces cellular stress response.[34] We designed a method to separate cell seeding from hydrogel formation in order to mitigate this stressor. First, the gellan gum−collagen IPN hydrogel scaffold was freeze-dried to form a porous dried network (Figure S3). Next, the harvested ADSC was resuspended in trehalose-containing cryomedia before being collectively infused into the freeze-dried hydrogel scaffold. A previous study has shown that cells displayed 75% higher viability when they were exposed to trehalose before encapsulation as compared to adding trehalose after the cells had already been encapsulated.[28] However, this method is only feasible if the hydrogel's mechanical properties remain unchanged throughout the freeze-drying process.

Unfortunately, by adjusting the freezing and drying rates, freeze-drying could become a "green" method to induce hydrogel porogenesis,[35] whereby a more porous matrix could be obtained when ice expands during the sublimation process.[36] In some studies, the increased hydrogel porosity was associated with drastically altered rheological properties.[37] Therefore, visual inspection and rheometry were conducted on our hydrogels to ensure they possess similar mechanical properties before and after freeze-drying. Based on the visual mechanical inspection, the freeze-drying process did not alter the ability of hydrogels to rehydrate and return to their original shape (Figure 2A).

For rheometry, amplitude sweeps were conducted, which determined the limit of linear viscoelasticity (LVE) of both hydrogels before and after freeze-drying to be 0.5% shear strain (Figure 2B), below which the hydrogels are sheared within a nondestructive deformation range. This percentage of shear strain was then fixed for subsequent frequency sweeps at 25 °C. Our results showed that the storage moduli (G′) of the hydrogels before and after freeze-drying were not statistically significantly different ($p > 0.05$) at an angular frequency of 1 Hz (Figure 2C). Furthermore, G′ was more than G″ throughout the entire angular frequency test range. This indicated that the hydrogels retained their stable gel-like properties of a viscoelastic solid before and after freeze-drying. Given that the mechanical properties of hydrogels have a significant influence on the cellular behavior,[38] the maintenance of mechanical robustness of the gellan gum-based

https://doi.org/10.1021/acs.biomac.2c00176
Biomacromolecules 2022, 23, 2803−2813

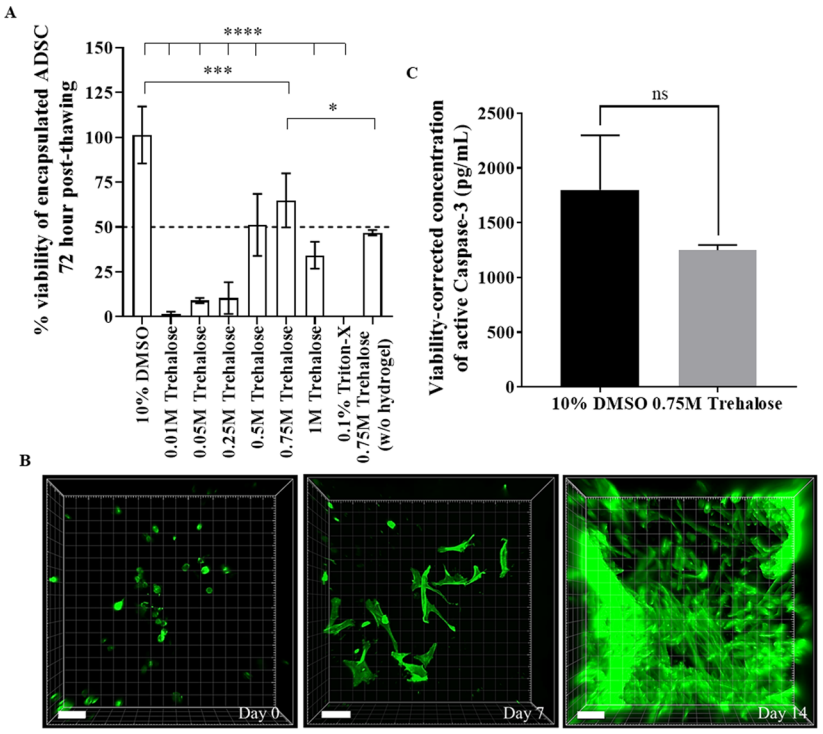

Figure 3. Biological evaluation following cryopreservation of ADSC-laden gellan gum−collagen hydrogels using trehalose. (A) Cell viability of encapsulated ADSCs cryopreserved with 10% DMSO or varying concentrations of trehalose determined 72 h after thawing. Cell viability was quantified using the MTS assay, and percentage cell viabilities were expressed against that of 10% DMSO. Data are presented as mean ± SD, $n = 3$, $^{*}p < 0.05$, $^{***}p < 0.001$, and $^{****}p < 0.0001$. The cell viability of nonencapsulated ADSCs cryopreserved with 0.75 M trehalose (without hydrogels) was also determined in the same manner. (B) 3D confocal images of encapsulated ADSCs F-actin (cytoskeleton)-stained in green with the Phalloidin-iFluor 488 reagent. Z-stacked images were captured with CLSM using a Zeiss LSM 710 to analyze the change in the cell morphology and density in the entirety of the cell-laden hydrogels at referred time points. Cell adhesion to, and cell spread within, IPN hydrogels could be observed in all three dimensions (scale bar: 100 μm). (C) Quantification of intracellular human active caspase-3 expressed by encapsulated ADSCs after 48 h of culture with 10% DMSO or 0.75 M trehalose. A higher concentration (1800.87 vs 1250.43 pg/mL) of active caspase-3 could be detected when cryopreserved ADSCs were cultured with 10% DMSO compared to 0.75 M trehalose. Data are presented as mean ± SD and $n = 3$.

hydrogel after freeze-drying renders it suitable for our modified cell encapsulation approach.

3.1.2. 3D Porosity. To determine if the internal structures of hydrogels were altered by freeze-drying, μCT imaging was conducted on hydrogels before and after freeze-drying. Figure 2D shows that the reconstructed 3D images of the hydrogel before and after freeze-drying appeared similar, with no significant change in the percentage porosity within the hydrogels ($p > 0.05$) (Figure S4). Its porosity is reported to influence the diffusion and exchange of waste and nutrients for normal homeostasis of encapsulated cells.[39] Hence, our data demonstrate that the freeze-drying process did not alter our hydrogel's cell-conducive microarchitecture.

3.1.3. Swelling Ratio and Degradation of Hydrogels in Cryomedia. The weight of freeze-dried hydrogels increased by ∼7× (∼700%) of their original weights when immersed in cryomedia containing 0.75 M trehalose (Figure 2E). This indicated that the freeze-dried hydrogels were able to absorb hydrophilic components, including solvents, of the cryomedia and rehydrate into a hydrophilic gel-like ECM-mimic. This is consistent with a previous study that demonstrated the freeze-dried low-acyl gellan gum hydrogels' ability to be completely rehydrated when its concentration was ≤1.5% (w/v).[40] It is important to note that freeze-dried hydrogels would require at least 30 min to reach equilibrium swelling after they were incubated in cryomedia containing 0.75 M trehalose. Therefore, if there was no preincubation, ADSCs suspended in the cryomedia would have a much lower tendency to be encapsulated by the partially swollen hydrogels and be left over in the liquid content within the cryovial. This would result in a lower cell number being encapsulated within the hydrogel network and hence lower cell viability after the cell-laden hydrogels were thawed (Figure S5).

After reaching equilibrium swelling, the fully swollen hydrogels were able to degrade in a timely fashion, losing more than 50% of their initial weights after ∼6 days of incubation (Figure 2F). This result demonstrated the biodegradable nature of our trehalose-infused hydrogel formula.

3.2. Biological Evaluation of Encapsulated ADSCs after Cryopreservation with Trehalose. *3.2.1. Cell Viability and Proliferation of Cryopreserved ADSCs Encapsulated within the Gellan Gum−Collagen Hydrogels.* The optimal concentration of trehalose to dehydrate encapsulated cells needs to be determined for different hydrogel cryopreservation systems.[2] This is because the molecular configurations and microstructures of hydrogels, which may affect the microenvironment-free water content, can differ considerably.[37] For our gellan gum−collagen hydrogel system, the post-thaw viability of encapsulated cells cryopreserved with varying trehalose concentrations was evaluated using the MTS assay. Figure 3A shows that a concentration of 0.75 M trehalose resulted in a recovery of 64.83 ± 15.08% of encapsulated cells 72 h after thawing as compared to 10%

https://doi.org/10.1021/acs.biomac.2c00176
Biomacromolecules 2022, 23, 2803−2813

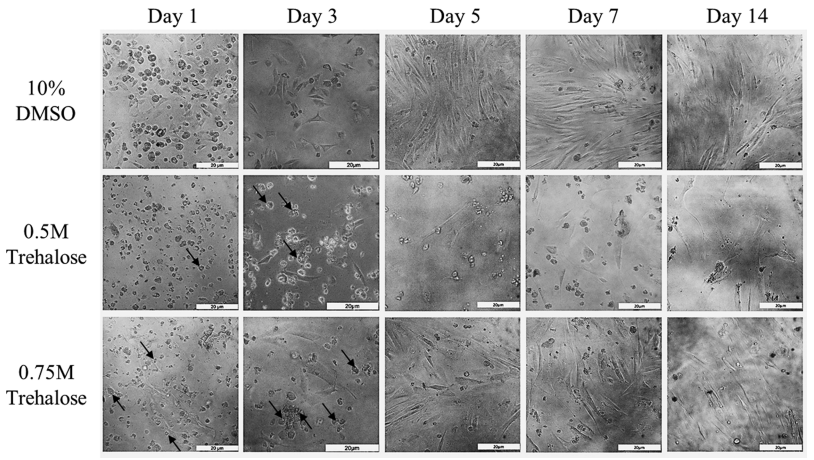

Figure 4. Phase-contrast microscopic images of the ADSC morphology and cell density over 1, 3, 5, 7, and 14 days of post-thawing. Encapsulated ADSCs were thawed along with the hydrogels and collectively transferred into cell culture plates. Cell-laden hydrogels were cryopreserved with 10% DMSO, 0.5 M trehalose, or 0.75 M trehalose. Characteristics bright vacuoles due to fluid-phase endocytosis-mediated cellular uptake of trehalose could be observed (dark arrows) (scale bar: 20 μm).

DMSO. In the absence of the IPN hydrogel, however, nonencapsulated ADSCs cryopreserved with 0.75 M trehalose only maintained 46.79 ± 1.459% of cell viability ($p < 0.05$). This result demonstrated that the IPN hydrogel worked synergistically with trehalose to provide added cryoprotection for the encapsulated ADSCs. On the other hand, in the presence of a very low concentration (0.01 M) of trehalose, minimal cryoprotection was conferred (Figure 3A). Therefore, a similar low cell viability is to be expected when encapsulated ADSCs are going to be cryopreserved without any cryoprotectant.

Beyond 0.75 M, at 1 M trehalose, cell dehydration occurred too rapidly and the percentage viability of encapsulated ADSCs declined sharply. This observation fits Mazur's theory of two-factor hypothesis; intracellular water needs to be reduced to prevent IIF but not excessively to avoid cell volume excursions during the freeze−thaw process.[41] Even at its optimal concentration, a significantly lower percentage of cell viability was observed when the encapsulated cells were cryopreserved with 0.75 M trehalose compared to 10% DMSO (Figure 3A). Nonetheless, given the noncell penetrative and hence trehalose's lower cryoprotective properties, our result is consistent with an existing study that evidences the use of trehalose as the sole CPA to cryopreserve hMSC-containing nanofibrous constructs.[40]

Three-dimensional (3D) confocal images of F-actin-stained ADSCs were also recorded to provide visual evidence of successful cell adhesion and migration within the 3D matrix of the hydrogels. Viable encapsulated ADSCs were observed to transform from a round morphology immediately after thawing to an elongated morphology with rapidly increasing cell density after 7 and 14 days of culture (Figure 3B). In contrast to the usual cryopreservation protocol, trehalose was not removed from the ADSC-laden gellan gum-based hydrogels immediately after thawing in this study. This simulates the situation in which the tissue constructs are implanted directly into the patient body. Therefore, the results showing successful cell adhesion and migration demonstrate the cell-conducive microenvironment of our trehalose-infused hydrogel cryopreservation system. Such a microenvironment would allow both the encapsulated ADSCs and the host cells to populate the entirety of the freeze-dried hydrogels after administration into the patient body despite the possibility of an initial heterogenic distribution of encapsulated ADSCs. Thus, this allows the freeze-dried ADSC-laden hydrogels to serve adequately as a synthetic scaffold for tissue engineering applications.

3.2.2. Quantification of Intracellular Human Active Caspase-3 of Cryopreserved ADSCs upon Continual Exposure to Trehalose. Human active caspase-3 is an intracellular enzyme secreted to cleave and activate other caspase enzyme family in the apoptosis signaling cascade.[42] ELISA revealed that after 48 h of incubation, 10% DMSO (1800.87 ± 498.2 pg./mL) induced a larger number of encapsulated ADSCs to undergo apoptosis compared to trehalose (1250.43 ± 47.47 pg./mL) ($p > 0.05$) (Figure 3C). However, there is no statistically significant difference between cells cryopreserved with 10% DMSO or 0.75 M trehalose in terms of caspase-3 production, which only suggests that trehalose could be an alternative to 10% DMSO to cryopreserve ADSC-laden hydrogels. As such, more studies are required to evaluate trehalose as a suitable sole CPA for other TERM constructs, in particular, tissue engineering scaffolds made from US FDA-approved biomacromolecules such as alginates as well as synthetic polymers such as polyethylene glycol, polylactic acid, and polycaprolactone.

3.2.3. Phase-Contrast Images of Cryopreserved ADSCs. Apart from biocompatibility, upon implantation, the scaffold should degrade in a timely fashion and release the encapsulated ADSCs for eventual assimilation with the surrounding damaged tissues for regeneration.[43] Encapsulated ADSCs, purported to have been gradually released from the hydrogels during degradation, were also observed to have attached onto the tissue culture polystyrene (TCPS) surface of the cell culture plates (Figure 4). Moreover, gradual elongation from a round morphology to the ADSC normal fibroblastic morphology could be observed for viable cells during days 1−5 of culture. This observation was made for all encapsulated cells, cryopreserved either with 10% DMSO, 0.5 M trehalose, or 0.75 M trehalose. Together with the results from the gravimetric analysis of the hydrogels (Figure 2F), biodegradability of our cryopreserved tissue construct was illustrated.

More importantly, characteristic intracellular vacuoles due to endocytosis of trehalose were also observed in ADSCs cryopreserved with trehalose post-thawing (Figure 4). For

https://doi.org/10.1021/acs.biomac.2c00176
Biomacromolecules 2022, 23, 2803−2813

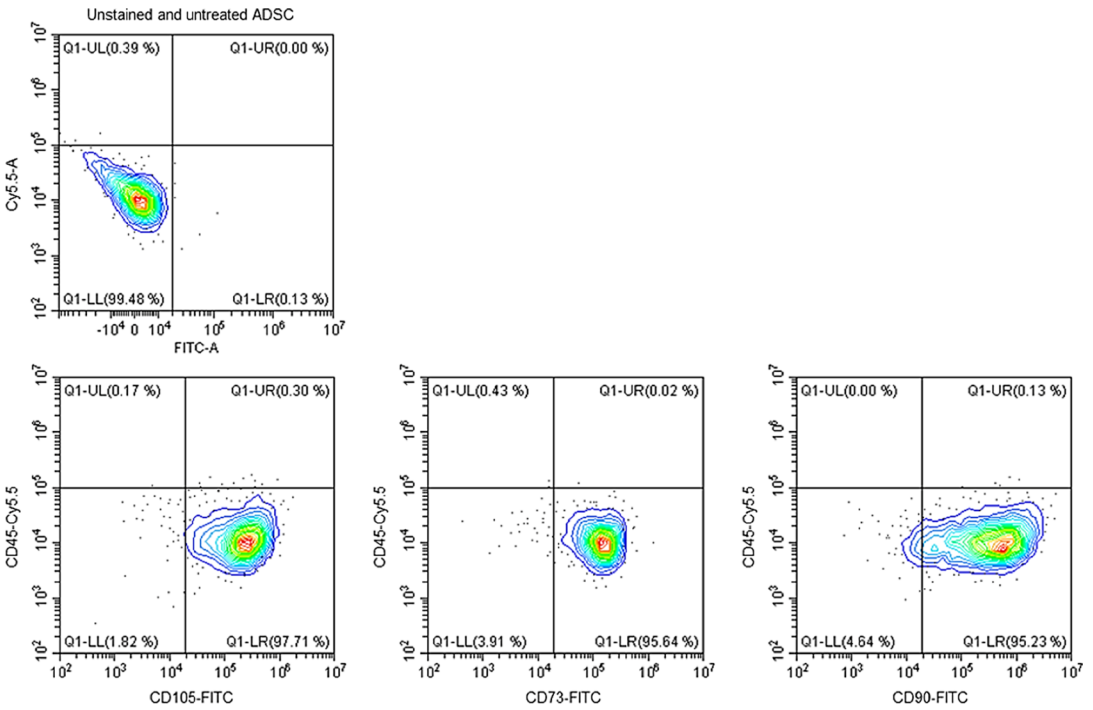

Figure 5. Flow cytometry analysis of encapsulated ADSCs cryopreserved with 0.75 M trehalose. The analysis was performed with gates set on CD73/90/105 + CD45 cell population. Representative flow cytometry contour plots showed that a majority of the cell population (>95%) expressed canonical CD73, CD90, and CD105 MSC surface markers, whereas a negligible population (<2%) of cell population was positive for the haemopoietic stem cell surface marker, CD45. This indicated that the cell phenotype of the ADSC was retained after cryopreservation with 0.75 M trehalose. A contour plot of untreated and unstained ADSCs denotes how the quadrants were drawn.

cell-impermeant trehalose,[44] cellular uptake is largely attributed to a process known as clathrin-dependent fluid-phase endocytosis.[45] This is a natural cellular phenomenon whereby cells were observed to internalize random loads of extracellular fluids to probe the environment.[46] If the extracellular fluid contained a high concentration of trehalose, a study has reported a cellular uptake of up to 55% of trehalose.[47] The presence of intracellular vacuoles only in cells cryopreserved with trehalose (0.5 or 0.75 M) indicated that clathrin-dependent fluid-phase endocytosis likely occurred when the trehalose-infused ADSC-laden hydrogels were preincubated at 37 °C under mild agitation for 30 min. The 30 min of preincubation time was selected based on the results of our preliminary study (Figure S5) as well as a prior study which found that significantly higher post-thaw cell viability was achieved for encapsulated stem cells when they were preincubated with 10% DMSO for 30 min.[48]

In addition to facilitating trehalose cellular uptake, the preincubation step allows sufficient time for trehalose to diffuse and interact with both the gel network and cells. This is particularly important for supramolecular hydrogel cryopreservation systems where a strong gel−trehalose−cell membrane interaction is needed to significantly reduce free water freezing content.[49] Trehalose is known to displace water molecules and form a stabilizing structure on cell membranes.[50] The strong gel−trehalose−cell membrane interaction may have augmented this effect and prevented ADSCs' membrane phospholipids from denaturing via desiccation when extracellular water crystallizes.[51] Collectively, these delineates how our reinvented method of using trehalose and a hydrogel cryopreservation system resulted in a slightly superior post-thaw cell viability as compared to both encapsulated ADSCs cryopreserved with other hydrogel systems[6] and nonencapsulated ADSCs cryopreserved with trehalose only (Figure 3A).

3.3. Cell Phenotype of Encapsulated ADSCs after Cryopreservation with 0.75 M Trehalose. To confirm that cryopreservation with 0.75 M trehalose did not adversely affect the stemness of encapsulated ADSCs, their cell phenotype was analyzed. We performed flow cytometry using specific antibodies against ADSC's canonical cell surface markers. Based on Figure 5, the cryopreserved ADSCs maintained a mesenchymal stem-like phenotype. The majority of ADSCs (>95%) were shown to express classical mesenchymal stem cell (MSC) markers CD73, CD90, and CD105, while a negligible population (<2%) expressed the hematopoietic marker CD45. Maintenance of putative MSC markers indicated the conservation of ADSC multipotency when 0.75 M trehalose was employed for cryopreserving the ADSC-laden hydrogel formula.

3.4. Osteogenic Differentiation Potential of Encapsulated ADSCs after Cryopreservation with 0.75 M Trehalose. To ascertain if the cryopreservation of encapsulated ADSCs with 0.75 M trehalose would affect their multipotent differentiation capacity, we sought to induce their osteogenic differentiation after cryopreservation. Based on Figure 6A, red streaks indicative of ARS-stained calcium deposits were clearly visible on the bottom surfaces of the culture plate wells after cells were incubated with osteogenic media, whereas wells remained clear for the groups of cells incubated in basal culture media. Quantitatively, cryopreservation of encapsulated ADSCs with either 0.5 M trehalose or 0.75 M trehalose did not affect subsequent levels of stem cell differentiation and mineralization (Figure 6B). The amount of alizarin red-stained calcium nodules extracted with 10% CPC was not statistically significantly different for encapsulated cells

https://doi.org/10.1021/acs.biomac.2c00176
Biomacromolecules 2022, 23, 2803−2813

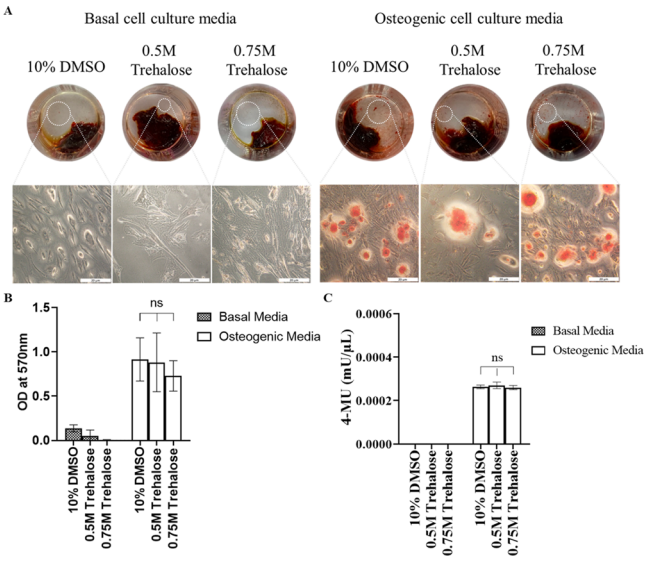

Figure 6. Osteogenic differentiation of encapsulated ADSCs after cryopreservation. (A) Qualitative images of ARS-stained calcium nodules, taken as gross images of the well, and microscopic images. ADSCs within the hydrogel were either incubated in basal culture media or induced toward osteogenic differentiation for 14 days after cryopreservation with either 10% DMSO, 0.5 M trehalose, or 0.75 M trehalose. Cryopreserved ADSCs, purportedly released from the hydrogels, were observed to have attached onto the TCPS surface of the cell culture plates. Alizarin red staining was done to identify calcium deposits (dotted white circles) secreted by successfully differentiated cells (scale bar = 20 μm). (B) Quantification of ARS-stained calcium nodules by measuring the blank-corrected absorbance of their CPC extract at 570 nm. (C) Quantification of intracellular ALP after osteogenic differentiation for 5 days by measuring the blank-corrected fluorescence of 4-MU. Data are presented as mean ± SD, $n = 2$, and $^{ns}p > 0.05$.

cryopreserved with 10% DMSO, 0.5 M, or 0.75 M trehalose ($p > 0.05$). The amount of intracellular ALP also did not differ significantly between ADSC cryopreserved with 10% DMSO, 0.5 M or trehalose, 0.75 M trehalose ($p > 0.05$) (Figure 6C).

According to the International Society for Cellular Therapy (ISCT), there are three minimum criteria to define mesenchymal stem cells, namely, (1) matrix adherence when maintained in standard culture conditions, (2) expression of canonical MSC surface markers CD105, CD73, and CD90 as well as lack of expression of the hematopoietic stem cell marker CD45, and (3) the ability to differentiate down the osteogenic, adipogenic, and chondrogenic lineages.[52] After cryopreservation with 0.75 M trehalose, the encapsulated ADSCs were shown to fulfill the first two criteria (Figures 3, 4 and 5B). Although cryopreserved ADSCs were not induced to undergo the adipogenic and chondrogenic pathways, their successful osteodifferentiation (Figure 6) is sufficient to demonstrate that the cryopreservation procedure did not induce undirected stem cell differentiation and did not alter the ADSC's differentiation potential. This is because it has been widely reported that both terminally differentiated ADSC and ADSC with altered differentiation potential cannot be induced to undergo any differentiation pathways.[53,54] Therefore, the results proved that our cryopreservation procedure did not affect ADSC's plasticity and, together with the low immunogenicity of gellan gum and collagen,[1] the cryopreservable hydrogel formula may possess immune privilege properties and fit the needs of a wide patient base.

4. CONCLUSIONS

In this study, we developed a method to incorporate trehalose, a biocompatible natural carbohydrate, into a gellan gum–collagen hydrogel to form an off-the-shelf polysaccharide cryopreservation system. The trehalose-infused hydrogel construct served as a proof of concept that synthetic tissues can be centrally fabricated and cryopreserved for subsequent delivery to off-site TERM institutions. Trehalose was incorporated into the hydrogel construct via a modified cell encapsulation process, which included a favorable preincubation step before cryopreservation. Compared to cryopreserving ADSCs without the hydrogel, the trehalose-infused hydrogel accorded significantly higher post-thaw cell viability. In addition, trehalose did not need to be removed after thawing. When the trehalose-infused ADSC-laden hydrogels were thawed and cultured, cryopreserved ADSC retained their stem cell-like phenotype as well as osteogenic potential. This suggested that the trehalose-infused ADSC-laden hydrogel could function as an off-the-shelf synthetic tissue designed for human body direct implantation. Moving forward, we envision in vivo evaluation of the cryopreservable synthetic construct to ascertain its safety and efficacy at an organism-level TERM model.

■ ASSOCIATED CONTENT

Supporting Information

The Supporting Information is available free of charge at https://pubs.acs.org/doi/10.1021/acs.biomac.2c00176.

Calibration curve for human active caspase-3 ELISA, calibration curve for ALP assay, hydrogel matrix microstructure imaging via scanning electron microscopy, quantification of the hydrogel porosity before and after freeze-drying using μ-CT, and cell viability of cryopreserved ADSCs when 10% DMSO was added into freeze-dried hydrogels with or without 30 min of subsequent incubation (PDF)

■ AUTHOR INFORMATION

Corresponding Author

Pui Lai Rachel Ee − *Department of Pharmacy, Faculty of Science, National University of Singapore, Singapore 117544, Singapore; NUS Graduate School for Integrative Sciences and Engineering, Singapore 119077, Singapore;* orcid.org/0000-0002-7277-6233; Phone: +65 6516 2653; Email: phaeplr@nus.edu.sg; Fax: +65 6779 1554

Authors

Jian Yao Ng − *Department of Pharmacy, Faculty of Science, National University of Singapore, Singapore 117544, Singapore*

Kee Ying Fremi Tan − *Department of Pharmacy, Faculty of Science, National University of Singapore, Singapore 117544, Singapore*

Complete contact information is available at: https://pubs.acs.org/10.1021/acs.biomac.2c00176

Author Contributions

J.Y.N. conceptualized, designed, and wrote the manuscript. J.Y.N. and K.Y.F.T. collected and analyzed the data. P.L.R.E. conceptualized, designed, edited, and supervised the work.

https://doi.org/10.1021/acs.biomac.2c00176
Biomacromolecules 2022, 23, 2803−2813

Funding

The authors would like to acknowledge research funding and facilities provided by the National University of Singapore and Ministry of Education Academic Research Fund (R148000287114) awarded to P.L.R.E. and NUS-IRP Scholarship to J.Y.N.

Notes

The authors declare no competing financial interest.

■ ACKNOWLEDGMENTS

We thank Ms. Sylvia Chew Yu Ting and co-workers, from the YLLSOM Confocal Microscopy Unit, for their help with 3D confocal imaging. We extend our appreciation to Mr. Manguiat Rex Malabanan and co-workers, from MD2 (NUS Institutional Animal Care and Use Committee (IACUC)), for their assistance with μ-CT scans.

■ ABBREVIATIONS

3D, three dimension; μCT, microcomputed tomography; ADSC, adipose-derived stem cell; ARS, alizarin red S; CD, cluster of differentiation; CLSM, confocal laser scanning microscopy; CPA, cryoprotective agent; CPC, cetylpyridinium chloride; DMEM, Dulbecco's modified Eagle's medium; DMSO, dimethyl sulfoxide; ECM, extracellular matrix; ELISA, enzyme-linked immunosorbent assay; FITC, fluorescein isothiocyanate; GG, gellan gum; IPN, interpenetrating network; IIF, intracellular ice formation; ISCT, international society for cellular therapy; LVE, limit of linear viscoelasticity; MSC, mesenchymal stem cell; MTS, (3-(4,5-dimethylthiazol-2-yl)-5-(3-carboxymethoxyphenyl)-2-(4-sulfophenyl)-2H-tetrazolium); PBS, phosphate buffered saline; PCL, polycaprolactone; Pe/Cy5.5, phycoerythrin/cyanine-5.5; PEG, polyethylene glycol; PLLA, polylactic acid; PES, polyether sulfone; PFA, paraformaldehyde; SEM, scanning electron microscopy; TCPS, tissue culture polystyrene; TERM, tissue engineering and regenerative medicine

■ REFERENCES

(1) Ng, J. Y.; Obuobi, S.; Chua, M. L.; Zhang, C.; Hong, S.; Kumar, Y.; Gokhale, R.; Ee, P. L. R. Biomimicry of microbial polysaccharide hydrogels for tissue engineering and regenerative medicine—A review. *Carbohydr. Polym.* **2020**, *241*, No. 116345.

(2) Trainor, N.; Pietak, A.; Smith, T. Rethinking clinical delivery of adult stem cell therapies. *Nat. Biotechnol.* **2014**, *32*, 729—735.

(3) Pegg, D. E., Principles of cryopreservation. In *Cryopreservation and freeze-drying protocols*; Springer, 2007; pp 39—57.

(4) Jang, T. H.; Park, S. C.; Yang, J. H.; Kim, J. Y.; Seok, J. H.; Park, U. S.; Choi, C. W.; Lee, S. R.; Han, J. Cryopreservation and its clinical applications. *Integr. Med. Res.* **2017**, *6*, 12—18.

(5) Li, Z.; Shen, L.; Huang, Y.; Xiang, X.; Zhao, G.; Luan, J. Water-transport and intracellular ice formation of human adipose-derived stem cells during freezing. *J. Therm. Biol.* **2020**, *93*, No. 102689.

(6) Weng, L.; Beauchesne, P. R. Dimethyl sulfoxide-free cryopreservation for cell therapy: A review. *Cryobiology* **2020**, *94*, 9—17.

(7) Zambelli, A.; Poggi, G.; Da, G. P.; Pedrazzoli, P.; Cuomo, A.; Miotti, D.; Perotti, C.; Preti, P. Clinical toxicity of cryopreserved circulating progenitor cells infusion. *Anticancer Res.* **1998**, *18*, 4705—4708.

(8) Stroncek, D.; Fautsch, S. K.; Lasky, L.; Hurd, D.; Ramsay, N.; McCullough, J. Adverse reactions in patients transfused with cryopreserved marrow. *Transfusion* **1991**, *31*, 521—526.

(9) Alessandrino, E.; Bernasconi, P.; Caldera, D.; Colombo, A.; Bonfichi, M.; Malcovati, L.; Klersy, C.; Martinelli, G.; Maiocchi, M.; Pagnucco, G. Adverse events occurring during bone marrow or peripheral blood progenitor cell infusion: analysis of 126 cases. *Bone Marrow Transplant.* **1999**, *23*, 533—537.

(10) Bauwens, D.; Hantson, P.; Laterre, P.-F.; Michaux, L.; Latinne, D.; De Tourtchaninoff, M.; Cosnard, G.; Hernalsteen, D. Recurrent seizure and sustained encephalopathy associated with dimethylsulfoxide-preserved stem cell infusion. *Leuk. Lymphoma* **2005**, *46*, 1671—1674.

(11) Junior, A.; Arrais, C.; Saboya, R.; Velasques, R.; Junqueira, P.; Dulley, F. Neurotoxicity associated with dimethylsulfoxide-preserved hematopoietic progenitor cell infusion. *Bone Marrow Transplant.* **2008**, *41*, 95—96.

(12) Guerreiro, B. M.; Freitas, F.; Lima, J. C.; Silva, J. C.; Dionísio, M.; Reis, M. A. Demonstration of the cryoprotective properties of the fucose-containing polysaccharide FucoPol. *Carbohydr. Polym.* **2020**, *245*, No. 116500.

(13) Fahy, G. M. Cryoprotectant toxicity neutralization. *Cryobiology* **2010**, *60*, S45—S53.

(14) Olsson, C.; Jansson, H.; Swenson, J. The role of trehalose for the stabilization of proteins. *J. Phys. Chem. B* **2016**, *120*, 4723—4731.

(15) Bumbat, M.; Wang, M.; Liang, W.; Ye, P.; Sun, W.; Liu, B. Effects of Me2SO and Trehalose on the Cell Viability, Proliferation, and Bcl-2 Family Gene (BCL-2, BAX, and BAD) Expression in Cryopreserved Human Breast Cancer Cells. *Biopreserv. Biobanking* **2020**, *18*, 33—40.

(16) Jung, S.-E.; Kim, M.; Ahn, J. S.; Kim, Y.-H.; Kim, B.-J.; Yun, M.-H.; Auh, J.-H.; Ryu, B.-Y. Effect of Equilibration Time and Temperature on Murine Spermatogonial Stem Cell Cryopreservation. *Biopreserv. Biobanking* **2020**, *18*, 213—221.

(17) Dovgan, B.; Barlič, A.; Knežević, M.; Miklavčič, D. Cryopreservation of human adipose-derived stem cells in combination with trehalose and reversible electroporation. *J. Membr. Biol.* **2017**, *250*, 1—9.

(18) Diaz-Dussan, D.; Peng, Y.-Y.; Sengupta, J.; Zabludowski, R.; Adam, M. K.; Acker, J. P.; Ben, R. N.; Kumar, P.; Narain, R. Trehalose-Based Polyethers for Cryopreservation and Three-Dimensional Cell Scaffolds. *Biomacromolecules* **2020**, *21*, 1264—1273.

(19) Awan, M.; Buriak, I.; Fleck, R.; Fuller, B.; Goltsev, A.; Kerby, J.; Lowdell, M.; Mericka, P.; Petrenko, A.; Petrenko, Y. Dimethyl sulfoxide: a central player since the dawn of cryobiology, is efficacy balanced by toxicity? *Regener. Med.* **2020**, *15*, 1463—1491.

(20) Shen, L.; Guo, X.; Ouyang, X.; Huang, Y.; Gao, D.; Zhao, G. Fine-tuned dehydration by trehalose enables the cryopreservation of RBCs with unusually low concentrations of glycerol. *J. Mater. Chem. B* **2021**, *9*, 295—306.

(21) Zhang, C.; Zhou, Y.; Zhang, L.; Wu, L.; Chen, Y.; Xie, D.; Chen, W. Hydrogel cryopreservation system: An effective method for cell storage. *Int. J. Mol. Sci.* **2018**, *19*, 3330.

(22) Zhao, G.; Liu, X.; Zhu, K.; He, X. Hydrogel Encapsulation Facilitates Rapid-Cooling Cryopreservation of Stem Cell-Laden Core—Shell Microcapsules as Cell—Biomaterial Constructs. *Adv. Healthcare Mater.* **2017**, *6*, No. 1700988.

(23) Casillo, A.; Parrilli, E.; Sannino, F.; Mitchell, D. E.; Gibson, M. I.; Marino, G.; Lanzetta, R.; Parrilli, M.; Cosconati, S.; Novellino, E. Structure-activity relationship of the exopolysaccharide from a psychrophilic bacterium: a strategy for cryoprotection. *Carbohydr. Polym.* **2017**, *156*, 364—371.

(24) Wang, J.; Salem, D. R.; Sani, R. K. Extremophilic exopolysaccharides: A review and new perspectives on engineering strategies and applications. *Carbohydr. Polym.* **2019**, *205*, 8—26.

(25) Chen, B.; Wright, B.; Sahoo, R.; Connon, C. J. A novel alternative to cryopreservation for the short-term storage of stem cells for use in cell therapy using alginate encapsulation. *Tissue Eng., Part C* **2013**, *19*, 568—576.

(26) Tang, M.; Chen, W.; Weir, M. D.; Thein-Han, W.; Xu, H. H. Human embryonic stem cell encapsulation in alginate microbeads in macroporous calcium phosphate cement for bone tissue engineering. *Acta Biomater.* **2012**, *8*, 3436—3445.

(27) Ng, J. Y.; Zhu, X.; Mukherjee, D.; Zhang, C.; Hong, S.; Kumar, Y.; Gokhale, R.; Ee, P. L. R. Pristine Gellan Gum—Collagen

Interpenetrating Network Hydrogels as Mechanically Enhanced Anti-inflammatory Biologic Wound Dressings for Burn Wound Therapy. *ACS Appl. Bio Mater.* **2021**, *4*, 1470−1482.
(28) Hara, J.; Tottori, J.; Anders, M.; Dadhwal, S.; Asuri, P.; Mobed-Miremadi, M. Trehalose effectiveness as a cryoprotectant in 2D and 3D cell cultures of human embryonic kidney cells. *Artif. Cells, Nanomed., Biotechnol.* **2017**, *45*, 609−616.
(29) Teramoto, N.; Sachinvala, N. D.; Shibata, M. Trehalose and trehalose-based polymers for environmentally benign, biocompatible and bioactive materials. *Molecules* **2008**, *13*, 1773−1816.
(30) Dou, M.; Lu, C.; Sun, Z.; Rao, W. Natural cryoprotectants combinations of l-proline and trehalose for red blood cells cryopreservation. *Cryobiology* **2019**, *91*, 23−29.
(31) Miyagi-Shiohira, C.; Kurima, K.; Kobayashi, N.; Saitoh, I.; Watanabe, M.; Noguchi, Y.; Matsushita, M.; Noguchi, H. Cryopreservation of adipose-derived mesenchymal stem cells. *Cell Med.* **2015**, *8*, 3−7.
(32) Elmore, S. Apoptosis: a review of programmed cell death. *Toxicol. Pathol.* **2007**, *35*, 495−516.
(33) Golub, E. E.; Boesze-Battaglia, K. The role of alkaline phosphatase in mineralization. *Curr. Opin. Orthop.* **2007**, *18*, 444−448.
(34) Nicodemus, G. D.; Bryant, S. J. Cell encapsulation in biodegradable hydrogels for tissue engineering applications. *Tissue Eng., Part B* **2008**, *14*, 149−165.
(35) Walker, J.; Santoro, M. Processing and production of bioresorbable polymer scaffolds for tissue engineering. In *Bioresorbable Polymers for Biomedical Applications*; Elsevier, 2017; pp 181−203.
(36) Grenier, J.; Duval, H.; Barou, F.; Lv, P.; David, B.; Letourneur, D. Mechanisms of pore formation in hydrogel scaffolds textured by freeze-drying. *Acta Biomater.* **2019**, *94*, 195−203.
(37) Sun, M.; Sun, H.; Wang, Y.; Sánchez-Soto, M.; Schiraldi, D. A. The relation between the rheological properties of gels and the mechanical properties of their corresponding aerogels. *Gels* **2018**, *4*, 33.
(38) Hadden, W. J.; Young, J. L.; Holle, A. W.; McFetridge, M. L.; Kim, D. Y.; Wijesinghe, P.; Taylor-Weiner, H.; Wen, J. H.; Lee, A. R.; Bieback, K.; Vo, B. N.; Sampson, D. D.; Kennedy, B. F.; Spatz, J. P.; Engler, A. J.; Choi, Y. S. Stem cell migration and mechanotransduction on linear stiffness gradient hydrogels. *Proc. Natl. Acad. Sci. U. S. A.* **2017**, *114*, 5647−5652.
(39) Byram, P. K.; Chaitanaya, K.; Barik, A.; Kaushal, M.; Dhara, S.; Chakravorty, N. Biomimetic silk fibroin and xanthan gum blended hydrogels for connective tissue regeneration. *Int. J. Biol. Macromol.* **2020**, *165*, 874−882.
(40) Cassanelli, M.; Norton, I.; Mills, T. Role of gellan gum microstructure in freeze drying and rehydration mechanisms. *Food Hydrocolloids* **2018**, *75*, 51−61.
(41) Mandal, A.; Clegg, J. R.; Anselmo, A. C.; Mitragotri, S. Hydrogels in the clinic. *Bioeng. Transl. Med.* **2020**, *5*, No. e10158.
(42) Porter, A. G.; Jänicke, R. U. Emerging roles of caspase-3 in apoptosis. *Cell Death Differ.* **1999**, *6*, 99−104.
(43) Griffin, D. R.; Archang, M. M.; Kuan, C.-H.; Weaver, W. M.; Weinstein, J. S.; Feng, A. C.; Ruccia, A.; Sideris, E.; Ragkousis, V.; Koh, J.; Plikus, M. V.; Di Carlo, D.; Segura, T.; Scumpia, P. O. Activating an adaptive immune response from a hydrogel scaffold imparts regenerative wound healing. *Nat. Mater.* **2020**, *20*, 560−569.
(44) Mutsenko, V.; Barlič, A.; Pezić, T.; Dermol-Černe, J.; Dovgan, B.; Sydykov, B.; Wolkers, W. F.; Katkov, I. I.; Glasmacher, B.; Miklavčič, D. Me2SO-and serum-free cryopreservation of human umbilical cord mesenchymal stem cells using electroporation-assisted delivery of sugars. *Cryobiology* **2019**, *91*, 104−114.
(45) Oliver, A. E.; Jamil, K.; Crowe, J. H.; Tablin, F. Loading human mesenchymal stem cells with trehalose by fluid-phase endocytosis. *Cell Preserv. Technol.* **2004**, *2*, 35−49.
(46) Kaksonen, M.; Roux, A. Mechanisms of clathrin-mediated endocytosis. *Nat. Rev. Mol. Cell Biol.* **2018**, *19*, 313.
(47) Zhang, M.; Oldenhof, H.; Sieme, H.; Wolkers, W. F. Freezing-induced uptake of trehalose into mammalian cells facilitates cryopreservation. *Biochim. Biophys. Acta, Biomembr.* **2016**, *1858*, 1400−1409.
(48) Khetan, S.; Corey, O. Maintenance of stem cell viability and differentiation potential following cryopreservation within 3-dimensional hyaluronic acid hydrogels. *Cryobiology* **2019**, *90*, 83−88.
(49) Lan, D.; Chen, X.; Li, P.; Zou, W.; Wu, L.; Chen, W. Using a novel supramolecular gel cryopreservation system in microchannel to minimize the cell injury. *Langmuir* **2018**, *34*, 5088−5096.
(50) Diaz, S.; Amalfa, F.; Biondi de Lopez, A.; Disalvo, E. Effect of water polarized at the carbonyl groups of phosphatidylcholines on the dipole potential of lipid bilayers. *Langmuir* **1999**, *15*, 5179−5182.
(51) Lynch, A. L.; Chen, R.; Slater, N. K. pH-responsive polymers for trehalose loading and desiccation protection of human red blood cells. *Biomaterials* **2011**, *32*, 4443−4449.
(52) Dominici, M.; Le Blanc, K.; Mueller, I.; Slaper-Cortenbach, I.; Marini, F.; Krause, D.; Deans, R.; Keating, A.; Prockop, D.; Horwitz, E. Minimal criteria for defining multipotent mesenchymal stromal cells. The International Society for Cellular Therapy position statement. *Cytotherapy* **2006**, *8*, 315−317.
(53) Bahsoun, S.; Coopman, K.; Akam, E. C. The impact of cryopreservation on bone marrow-derived mesenchymal stem cells: a systematic review. *J. Transl. Med.* **2019**, *17*, 397.
(54) Phinney, D. G.; Prockop, D. J. Concise review: mesenchymal stem/multipotent stromal cells: the state of transdifferentiation and modes of tissue repair−current views. *Stem Cells* **2007**, *25*, 2896−2902.

https://doi.org/10.1021/acs.biomac.2c00176
Biomacromolecules 2022, 23, 2803−2813